Structure and Picosecond Excited-States Dynamics in Isolated, Supercooled 4-(*N*,*N*-Dimethylamino)benzonitrile

F. Pérez Salgado,* J. Herbich,† A. G. M. Kunst, and R. P. H. Rettschnick

Laboratory for Physical Chemistry, University of Amsterdam, Nieuwe Achtergracht 127, 1018 WS Amsterdam, The Netherlands

Received: January 11, 1999

The first experimental evidence is presented for a strong coupling between electronic states in isolated, supercooled 4-(*N*,*N*-dimethylamino)benzonitrile, DMABN. In the fluorescence excitation spectrum, measured under isolated supercooled conditions, two types of transitions were found (B-type and C-type). Rotational contour analysis of the B-type bands ($\pi\pi^*$ character) shows that there is hardly any difference between the geometries of the ground and excited states; the molecule retains its planar conformation. In the out-of-plane transition (C-type band) the equilibrium position of the dimethylamino group twists 90° with respect to the benzonitrile part. The broadening of the rotational lines indicates that the fluorescence is preceded by a fast radiationless intramolecular process (internal conversion) on a picosecond time scale. For the B-type bands it was found that the broadening increases with the vibrational energy.

1. Introduction

DMABN, 4-(*N*,*N*-dimethylamino)benzonitrile, aroused the interest of Lippert[1] in 1962 because of its "anomalous" fluorescence in the presence of polar solvents. A second, strongly red-shifted emission band was found in addition to the primary fluorescence. The shift of this band as a function of the polarity of the solvent indicates that the emitting state is strongly polar. Grabowski et al.[2] explained the strong red shift in terms of a charge transfer in the molecule, accompanied by a twisting of the dialkylamino group. In polar solvents, an excited DMABN molecule undergoes a rotation of the dimethylamino group about the dimethylamino bond. Thus, it achieves a perpendicular geometry with respect to the plane of the benzene ring. This motion is accompanied by a charge separation, as evidenced by the measured increase of the dipole moment from 7.6 D in the ground state to 16.2 D in the excited state. The combined processes are called "TICT": twisted intramolecular charge transfer. This hypothesis was extended in the following years, and experimental evidence[3] was gathered; several molecules were found to exhibit similar behavior. Though the concept of TICT is now widely accepted, information on the structure of the excited states (the primarily excited and the TICT state) is scant. Much of the performed work, both in solution[4−7] and in a jet,[8] has focused on the interaction with the solvent. An important and partly unresolved aspect of the TICT mechanism is the relaxation of the directly excited state to the TICT state. The existence of a solvent-free mechanism has been established in some systems,[9] although not in DMABN, where the presence of highly polarizable solvents seems necessary to yield the dual fluorescence.

Accurate information concerning the excited state may be obtained by the study of isolated molecules in the cold gas phase. Laser supersonic molecular jet spectroscopy offers the following advantages: (1) the molecule is in a well-defined initial state because of the low internal temperatures for rotation and vibration; (2) the interaction with other molecules is minimized; (3) high spectral resolution can be obtained so that vibrations and structural changes in the excited state can be studied. Information about the dynamics of the excited state can be obtained through high-resolution fluoresence spectra.

Conformational changes in the molecule that may occur upon electronic excitation are an important aspect of the TICT mechanism. In the electronic spectra of jet-cooled isolated small molecules even rovibronic transitions can be distinguished. By analysis of the rotational band contours, conformational changes in the excited state can be traced and at the same time the direction of the transition dipole moment is determined.

In the gas phase and in apolar solvents, DMABN exhibits only fluorescence from the primarily excited state; the TICT fluorescence is found in polar surroundings. The maximum of the emission from the locally excited state in apolar solvents is centered at ∼340 nm. Also in the jet only fluorescence from the locally excited state was found[10,11] upon exciting the isolated molecule to 4500 cm^{-1} above the supposed 0−0 level. The excited state of isolated DMABN was investigated by Howells et al.,[12] Kobayashi et al.,[13] Gibson et al.,[14,15] and Grassian et al.[16] They elucidated some aspects of the vibrational spectrum as well as conformational aspects of the DMABN molecule in the excited state. The ground-state structure of isolated, jet-cooled DMABN has been determined by Kajimoto et al.[17] with microwave spectroscopy. According to their microwave experiment, the dihedral angle ϕ between the planes of the dimethylamino part and the benzonitrile part is 15° and the twist angle θ of both planes around the C−NMe_2 axis is 0° for the ground state of DMABN. In solution, Heine et al.[18] deduced a dihedral angle ϕ of 10.8° (293 K) or 11.9° (253 K). From X-ray diffraction, the dihedral angle and the twist angle were found to be both approximately 0° by Gourdon et al.[19] The structure in the excited state in the jet was deduced from high-resolution LIF excitation spectra measured in a supersonic free jet by Kajimoto et al.[17] and by Howells et al.[12] With rotational contour analysis of a transition in the excitation spectrum, Kajimoto et

* To whom correspondence should be addressed.
† Present address: Institute of Physical Chemistry, Polish Academy of Sciences, Kasprzaka 44, 01-244 Warsaw, Poland.

10.1021/jp990136n CCC: $18.00 © 1999 American Chemical Society
Published on Web 04/09/1999

al. found that the dihedral angle ϕ reduces to 0° upon electronic excitation while the twist angle θ has a value of 30° in the excited state. Howells et al. made similar rotational contour analyses; they point out that the identification of "one" single equilibrium geometry is rather difficult because the rotational contours of the vibronic bands differ slightly from each other in the onset of the excitation spectrum. Grassian et al.[16] calculated a value of 30° for the twist angle using a Franck−Condon intensity analysis for the peaks that were assumed to belong to the torsional motion in the LIF excitation spectrum, assuming 0° for the twist angle in the ground state. They calculated a dihedral angle of 0° for the excited state, using the same Franck−Condon procedure. Gibson[14,15] and Howells[12] report a lifetime of ∼5 ns for most transitions in isolated, jet-cooled DMABN.

From the theoretical side, semiempirical[20] and ab initio[21−23] quantum mechanical calculations have been conducted on the singlet states of DMABN. According to these calculations, the planar structure is the most stable one in the ground and excited states.

In this article we present new experimental material on the structure of DMABN in the excited state and on the nature of the excited state. Different types of transitions, B and C types, are found in the excitation spectrum, corresponding to different equilibrium conformations of DMABN in the excited state. Line-broadening data of these transitions in combination with high-resolution emission spectra are indicative of interaction between different excited electronic states.

2. Experimental Section

2.1. Materials. 4-(*N*,*N*-Dimethylamino)benzonitrile (Aldrich, 98%) was used without further purification.

2.2. Supersonic Beam Investigations. The expansion chamber was evacuated by a Roots pump (Edwards E4500, 500 m^3/h) backed by a rotary fore pump (Edwards E2M80, 80 m^3/h). A continuous supersonic jet was produced by expanding helium through the nozzle of the injector. The nozzle diameter was 100 μm. The background pressure in the expansion chamber was 0.1 mbar at a source pressure of 3 bar.

A pulsed dye laser (Lumonics HyperDYE-300) was used, pumped at 308 nm (XeCl) with an excimer laser (Lumonics HyperEX-460) operating at 80 Hz. The dye laser output was frequency-doubled (HyperTRAK-1000) with KD*P crystals. The spectral bandwidth was 0.15 cm^{-1} after frequency doubling. The pulse duration was 9 ns. The intensity of the UV jet was monitored by a calibrated EG&G radiometer and was between 10 and 100 mW. A hollow cathode neon discharge lamp was used for calibration of the wavelength of the dye laser. The accuracy of calibration was 0.1 cm^{-1} at 300 nm. The nonlinearity of the scanning was better than 1 pm over 1 nm.

The laser beam was sent into the vacuum chamber, using several quartz 90° prisms and a lens (focal length, 500 mm) to focus the beam in the supersonic jet.

Measurements were performed at distances between 10 and 40 nozzle diameters downstream of the nozzle. The distance is denoted as the reduced distance z_{red}, expressed in nozzle diameters. No change in excitation and emission spectra was achieved at reduced distances larger than $z_{red} = 15$. This means that no further cooling of the isolated molecule is achieved at distances larger than 15 nozzle diameters downstream of the nozzle. To obtain maximum signal intensity under the best cooling conditions, most experiments were performed at this distance ($z_{red} = 15$). For jet-cooled 4-(dimethylamino)benzonitriles and 4(dialkylamino)pyrimidines the rotational temperature in our setup is approximately 5 K.[8,24]

Laser-induced fluorescence (LIF) spectra were recorded from 310 to 350 nm. Dispersed fluorescence from the supersonic jet was collected with right-angle geometry by a spherical quartz condenser (Melles Griot 01MCP119, with a diameter of 50 mm and a focal length of 50 mm), which imaged via one or two mirrors onto the slit of a monochromator. The set up allowed the use of two monochromators. A Zeiss M20 grating monochromator was used to obtain low-noise excitation spectra. A Jobin-Yvon HR 11000 was used for high-resolution emission spectra (1200 grooves/mm; ultimate resolution of 0.008 nm). The absolute wavelength of the Zeiss monochromator was calibrated with a Na spectral lamp at 598.3 nm. The wavelength of the Jobin-Yvon HR 11000 was calibrated with the 312.57 or 302.15 nm line of a Hg spectral lamp. Using other lines from Hg, the nonlinearity of the wavelength scale was found to be better than 20 pm over a range of 250 nm.

The fluorescence was directed onto the photomultiplier (EMI S20, 9558QA). The signals from the photomultiplier were fed into a gated integrator and boxcar averager (SR 250) from Stanford Research Systems. The signal received from the photomultiplier was only sampled during a specific gate width (1 ms), which was timed using the trigger facility of the boxcar. Only signals from the photomultiplier corresponding to light arriving coincident with and slightly after the laser pulse were sampled. The signal-to-noise ratio increases as the square root of the number of samples. In most cases, 100 laser shots were integrated.

The signal from the boxcar was connected to a computer interface (SR 1245), which was controlled by a software package (SR 1265) run on an IBM AT personal computer. The spectral response of the detection system is almost constant within the wavelength range that is used in the experiments. For that reason we did not attempt to correct the high-resolution emission spectra for the wavelength dependence of monochromator transmission and photomultiplier efficiency. The excitation spectrum was corrected for fluctuations in dye laser intensity. The accuracy in peak positions was found to be better than 0.5 cm^{-1}. The line broadening in our setup due to the Doppler effect (distribution of molecular speeds perpendicular to the jet axis) is 0.05 cm^{-1}.

2.3. Rotational Contour Simulations. The rotational contours were simulated using a home-written[25] rotational contour program based on the asymmetric top rigid rotor approximation in which the interaction of rotation with electronic and vibrational motion is neglected. The rotational band contour is calculated and compared with the experimentally observed one. The program was checked for various asymmetric top molecules for which the structure is known: tetrazine,[26] the tetrazine−argon van der Waals complex,[27] benzonitrile−argon,[28] the benzonitrile−dimer,[29] aniline.[29,30]

The conformational parameters that may be adjusted in DMABN are the twist angle θ, the dihedral angle ϕ, the distance between the dimethylamino group and the benzonitrile part, r(C−NMe_2), the distance between the cyano group and the benzene ring, r(C−CN), and changes in the benzene ring. We departed from the ground-state structure of DMABN as determined by Kajimoto et al.[17] from microwave experiments. Benzonitrile part: 0.140 nm, C−C; 0.108 nm, C−H; 0.145 nm, C−CN; 0.1159 nm, C≡N. Bond angles of benzonitrile part: 120°, C−C−C; 120°, C−C−H. Dimethylamino part: 0.137 nm, C−NMe_2; 0.146 nm, N−CH; 0.108 nm, C−H. Bond angles for dimethylamino part: H−C−H, 120°; Me−N−Me, 115.7°,

TABLE 1: Rotational Constants *A*, *B*, and *C* (cm^{-1}) and κ (Asymmetry Parameter) of DMABN for Different Values of θ and ϕ[a]

twist angle θ	*A*	*B*	*C*	κ
(dihedral angle $\phi = 0$)				
0	0.115 090	0.019 259	0.016 600	−0.9460
30	0.115 090	0.019 071	0.016 743	−0.9526
60	0.115 090	0.018 593	0.017 129	−0.9701
90	0.115 090	0.018 198	0.017 479	−0.9852
(dihedral angle $\phi = 15$)				
0	0.115 600	0.019 064	0.016 485	−0.9480
30	0.115 609	0.018 883	0.016 622	−0.9543
60	0.115 630	0.018 428	0.016 992	−0.9709
90	0.115 641	0.018 059	0.017 318	−0.9849

[a] r(C−CN): 0.145 nm. r(C−NMe_2): 0.137 nm.

$\theta = 0°$, $\phi = 15°$. We used the same geometry of the benzene ring in both the ground and excited states and different values for the rest of the parameters in order to optimize the simulation of the observed contour. The following values of these parameters have been used: r(C−CN) = 0.145, 0.142, 0.149 nm. Dimethylamino part: dihedral angle $\phi = 0°$, 15°, 30°, 45°; twist angle $\theta = 0°$, 30°, 45°, 60°, 75°, 90°; r(C−NMe_2) = 0.137, 0.118, 0.130, 0.154 nm. From these structural parameters the rotational constants can be calculated. Some of the resulting values for the rotational constants are listed in Table 1.

To establish the rotational temperature of DMABN in the jet, we varied the rotational temperature in the simulations from 3 to 20 K. The best fits were obtained with a rotational temperature of 5 K at $z_{red} = 15$. Both for the B-type bands and the C-type band rotational band contours were measured at $z_{red} < 15$, where the cooling of the molecule is less. For the C-type band (at 0−0 + 136 cm^{-1}) the observed band could be well fitted with values for the rotational temperature of 15 K (at $z_{red} = 5$), 8−10 K (at $z_{red} = 7$), 6−7 K (at $z_{red} = 10$); for the B-type bands similar results were found.

2.4. Line Broadening and Excited-State Lifetime. The observed band contour is the envelope of the rovibronic transitions. Owing to molecular properties and the experimental setup, each line will be broadened. The line broadening due to the experimental setup is caused by the laser bandwidth and the Doppler effect. The broadening in our setup is approximately 0.16 cm^{-1} and will be Gaussian (inhomogeneous). Lifetime broadening is homogeneous and gives rise to a Lorentzian line profile. If there is no congestion and if the statistical limit approximation[31] is valid, the relation between the line width $\Delta\sigma_\tau$ of a transition and the excited-state lifetime τ is given by (with c and τ in cgs units) $\Delta\sigma_\tau = 1/(2\pi c\tau)$ (cm^{-1}).

The lifetimes in section 3 are calculated by the convolution of a Gaussian and a Lorentzian line shape. The value of the line width of the Gaussian line shape is fixed to 0.16 cm^{-1}, corresponding to the broadening of the experimental setup. It should be noted that the interpretation of the line shape can be troubled by congestion. Strongly congested band contours were not used for calculating lifetimes.

3. Results

3.1. Excitation Spectrum. Figure 1 presents the fluorescence excitation spectrum over the first 1200 cm^{-1} of isolated DMABN. The spectrum is characterized by a few intense peaks surrounded by many low-frequency transitions. The first transition, at 310.022 nm, is relatively weak. The intensities of all the peaks in this spectrum show exactly the same pressure and temperature dependence, and therefore, we conclude that no hot bands appear in this spectrum. It looks reasonable to ascribe

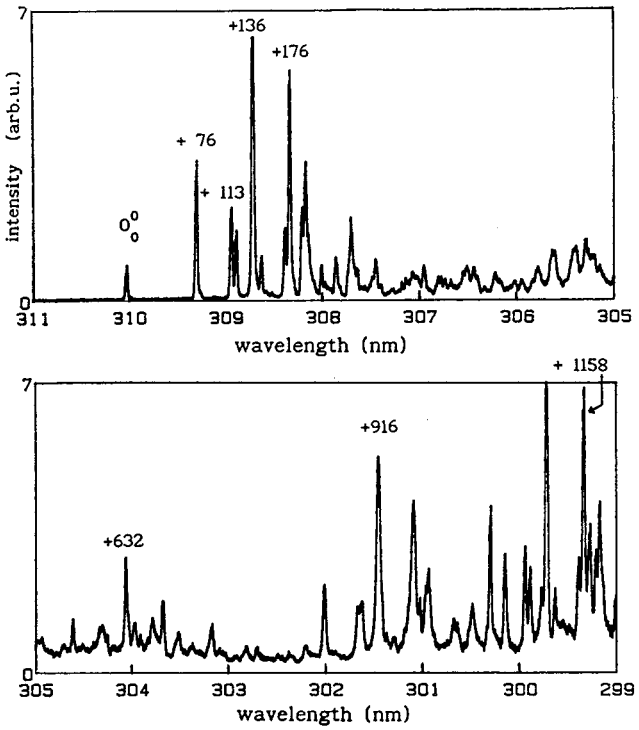

Figure 1. LIF excitation spectrum of DMABN at $z_{red} = 15$. The relative position (in cm^{-1}) of some transitions with respect to the 0−0 is indicated. The temperature of the sample before the expansion is 110 °C. The detection wavelength is 330 nm at a resolution of 1.6 nm fwhm. The pressure of the helium carrier gas is 3 bar.

the first peak at 310.022 nm (corresponding to $\nu_{vac} = 32\,246.55$ cm^{-1}) to the 0−0 transition. This is in accordance with the assignment given by Grassian et al.[16] (32 255.5 cm^{-1} in air) and Howells et al.[12] Kobayashi et al.[13] and Gibson et al.[14] report similar spectra; however, the relatively weak band at 310.022 nm is apparently too weak to be detected in their spectra. Table 2 summarizes the major transition frequencies and the relative peak intensities. These authors[12−16] have suggested that the low-frequency transitions in the excitation spectrum are due to both the twist motion and the inversion motion of the dimethylamino group, which implies that the equilibrium positions of the nuclei involved in these motions are different in the ground state and the excited electronic state.

3.2. Rotational Contours near the Origin. Most transitions in the 0−0 region have a double-headed B-type contour. In Figure 2 we show the band contour of the 0−0 + 176 cm^{-1} transition, which was also analyzed by Kajimoto et al.[17] The bands at 0−0 + 76 cm^{-1}, 0−0 + 118 cm^{-1}, 0−0 + 145 cm^{-1} and 0−0 + 171 cm^{-1} have the same rotational contour as the band at 0−0 + 176 cm^{-1}.

As already explained, analysis of the rotational contour yields information on the excited-state conformation of the molecule. To simulate the observed rotational contours, both a ground and an excited-state structure have to be assumed. For the ground-state structure we used the structure determined by Kajimoto et al. with microwave spectroscopy, in which the dihedral angle ϕ between the planes of the dimethylamino part and the benzonitrile part is 15° and the twist angle θ of both planes around the C−NMe_2 axis is 0°. For the excited state several values for ϕ, θ, R(C−CN), and r(C−NMe_2) were used (cf. Experimental Section).

The best fit is obtained if there is no difference between ground and excited states, neither in the twist angle θ nor in the dihedral angle ϕ and in the C−NMe_2 and C−CN distances.

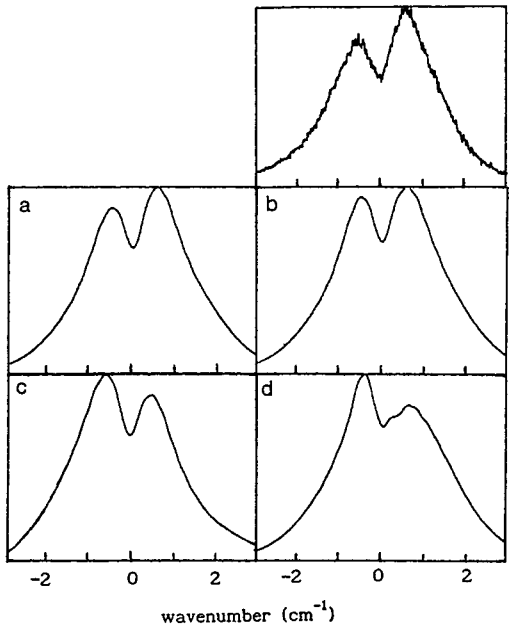

Figure 2. (upper right) Observed rotational band contour of the 0−0 + 176 cm^{-1} transition in isolated DMABN at $z_{red} = 15$. The detection wavelength is 330 nm, with the monochromator at a slit width of 1.76 nm fwhm. The band contour was independent of the laser power and the detection width (checked between 0.15 and 10 nm slit width fwhm). Simulated band contours of DMABN for the B-type transition with several values for the twist angle θ in the excited state are shown: (a) 0° → 0°; (b) 0° → 30°; (c) 0° → 60°; (d) 0° → 90°. The dihedral angle ϕ was taken 15° in both the ground and excited states. Simulation parameters are the following: $T_{rot} = 5$ K, Lorentzian line shape, fwhm = 0.3 cm^{-1}.

TABLE 2: Peak Positions and Intensities in the LIF Excitation Spectrum of DMABN (Wavenumbers in a Vacuum)

wavelength (nm)	wavenumber (cm^{-1})	Δ (cm^{-1})	intensity (arbitrary units)
310.022	32 246.5	0.0	0.71
309.292	32 322.6	76.1	2.68
308.937	32 359.7	113.2	1.75
308.887	32 365.0	118.5	1.07
308.716	32 382.9	136.4	6.32
308.631	32 392.0	145.3	0.69
308.386	32 417.7	171.1	1.30
308.336	32 422.9	176.4	5.65
308.206	32 436.6	190.1	1.78
308.171	32 440.3	193.7	3.10
307.707	32 489.1	242.6	2.06
304.607	32 819.7	573.2	1.34
304.058	32 879.1	632.6	2.87
303.667	32 921.4	674.8	1.75
303.162	32 976.2	729.7	1.10
302.006	33 102.4	855.9	2.18
301.646	33 142.0	895.4	1.44
301.455	33 162.9	916.4	5.18
301.085	33 203.7	957.1	4.25
300.945	33 219.1	972.7	2.06
300.655	33 251.2	1004.6	1.00
300.484	33 270.1	1023.5	1.46
300.144	33 307.8	1061.2	3.68
299.764	33 350.0	1103.5	7.14
299.273	33 404.7	1158.2	6.55

The rotational band contour simulation is *most sensitive to changes in the twist angle* θ. We have tried the following combinations: 0° → 0°; 0° → 30°; 0° → 60°; 0° → 90°. In Figure 2 the simulated contours with different twist angles θ are shown. We have also used values for the twist angle between the mentioned ones, but the recorded spectra do not allow for a higher degree of precision in the determination.

For the dihedral angle ϕ we have used the following values in the excited state: 0°, 15°, 30°, and 45°. The simulated contour is hardly sensitive to the dihedral angle ϕ. For the C−NME_2 and C−CN distances contractions or elongations of at most 15% of the value in the ground state were taken. For the used spectral resolution, the simulations were only slightly dependent on the variations in these parameters. The relative height of the P branch with respect to the R branch is mostly influenced by the twist angle. Changes in ϕ and the C−NMe_2 and C−CN distances affect mostly the total width of the P and R branches. The maximum differences in these parameters induce only small changes in the simulated contour, and the best fit is obtained if these parameters have the same values in the ground and excited states.

The best fits were obtained with Lorentzian line shapes; Gaussian line shapes result in far too low intensities in the wings of the bands. We have used a Lorentzian line profile with a width of 0.3 cm^{-1}. The band contours were also measured at other distances from the nozzle (see Experimental Section; only different values for the rotational temperature were necessary to fit the band contour). The total line broadening due to the experimental setup is approximately 0.16 cm^{-1} (due to laser bandwidth and Doppler effect). Since the line profile used in the simulation is Lorentzian, we interpret the remaining width as lifetime broadening (see Experimental Section). As explained in section 2.4, the lifetime can be estimated by the convolution of a Gaussian (0.16 cm^{-1}) and a Lorentzian line profile. If we assume that no congestion is present, this corresponds to a lifetime of approximately 24 ps. However, we can expect some congestion, which means that the 24 ps is a lower limit.

The rotational contour of the 0−0 band is slightly different from those of the B-type bands just mentioned. The wings are more narrow, and the indentation between the P and R branches is more pronounced for the 0−0 band. The best fit of the band at 0−0 is obtained with a Gaussian line profile if a width of 0.3 cm^{-1} fwhm is used in the simulation procedure instead of a Lorentzian line profile. There is no detectable Lorentzian broadening, which means that no lifetime can be deduced from the broadening of this transition. The band at 0−0 + 113 cm^{-1} (see Figure 5c) looks B-type, but it seems to be congested. It was not possible to make a suitable fit. We will come back to this in the next section.

We conclude that the investigated B-type transition in DMABN is not accompanied by any noticeable change in the molecular structure with respect to its ground-state structure. The dimethylamino moiety does not twist, or it twists only slightly upon excitation; the change is too small to be observed in the rotational contour. The progression of the low-frequency motion in the LIF excitation spectrum may be due to a slight change along the twist angle, but also a small change along some other coordinate may be responsible for it. The B-type transition is polarized along the short axis. The same type of transition is found in benzene with polar substituents, such as benzonitrile,[32] aniline,[28] and aniline derivatives,[33] *p*-fluoroaniline[34] and 4-aminobenzonitrile.[14,15] Small geometry changes in the ring or in the substitutes occur as a consequence of changes in the electron density upon electronic excitation. However, these changes are too small to be observed in the measured band contours. The B state will have, owing to the polarity of the molecule, some charge-transfer character, but mainly $\pi\pi^*$ character, due to the excitation of the benzenoid electrons. Because of the analogy between DMABN and the

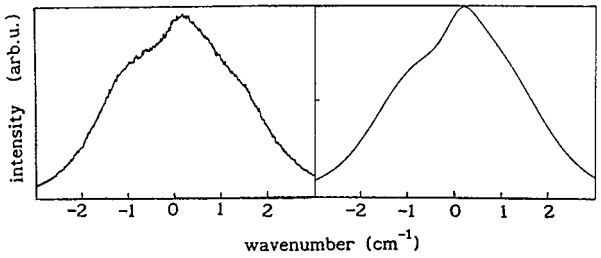

Figure 3. At the left the observed rotational contour of the C-type transition at $0-0 + 136$ cm^{-1} in DMABN. At the right the simulation with a change of 0° to 90° in the twist angle from the ground to the excited state. Other simulation parameters are the following: $T_{rot} = 5$ K, line shape Lorentzian, fwhm = 0.9 cm^{-1}.

molecules just mentioned, we expect that the B-type excitations in DMABN are localized on the benzonitrile part of the molecule and will have $\pi\pi^*$ character.

Surprisingly, not all transitions in the onset of the LIF excitation spectrum have a B-type contour. The transition at $0-0 + 136$ cm^{-1}, shown in Figure 3, has a *C-type contour* in which a prominent Q branch can be observed. In contrast to the B-type band, the C-type band is best simulated with a *large change in twist angle*, namely, 0° → 90°. Other combinations, 0° → 0° or 0° → 30°, do not fit mainly because the shape of the P and R branches do not coincide with that of the recorded $0-0$ spectrum. The fit for 0° → 60° is not as good as that for 0° → 90°. Changing other parameters, such as the dihedral angle ϕ, the R(C−CN), and r(C−NMe$_2$) distances, had little influence on the simulation.

The line broadening is markedly different from that of the B-type contours in the same spectral region. The C-type band can only be simulated using a Lorentzian line shape with a fwhm of 0.9 cm^{-1}. If there is no congestion, this corresponds to a lifetime of about 6.5 ps for this state. Some broadening due to spectral congestion will not have any considerable effect on the calculated lifetime. If we assume a broadening of, for example, 0.15 cm^{-1} due to congestion, then the lifetime would be 8 ps. In both cases the lifetime of this state is very short.

This transition is perpendicular to the molecular plane, and therefore, it must be an nπ^* transition. Since in the DMABN molecule the n orbital of the dimethylamino group and (one of) the π^* orbital(s) of the benzonitrile group are spatially quite separate, the nπ^* transition may involve an intramolecular charge transfer and thereby a large change in the dipole moment. In contrast to the B-type transition, where the excitation can be considered to be localized in the benzonitrile part, it is likely that the dimethylamino group is involved in the excitation to the C-type transition.

Both vibronic mixing and direct excitation to some other electronic state can explain the presence of the C-type band in the excitation spectrum. To make a choice between these two possibilities, additional experimental data are used in the next two sections.

3.3. Rotational Contours of Transitions at Higher Excess Energy. The higher-lying transitions exhibit broadened band contours. Parts a−h of Figure 4 display the band contours of some transitions, both in the $0-0$ region and at higher excess energy. Fits to the band contours at higher excess energy were only successful if high values for the band broadening are taken. Also, for these bands the best fits were obtained if Lorentzian line shapes are used. For the simulation of the contours different values for the line width had to be used, which are listed in Table 3. In Figure 5 the simulated rotational band contours are shown for B- and C-type bands using different values for the line width.[35]

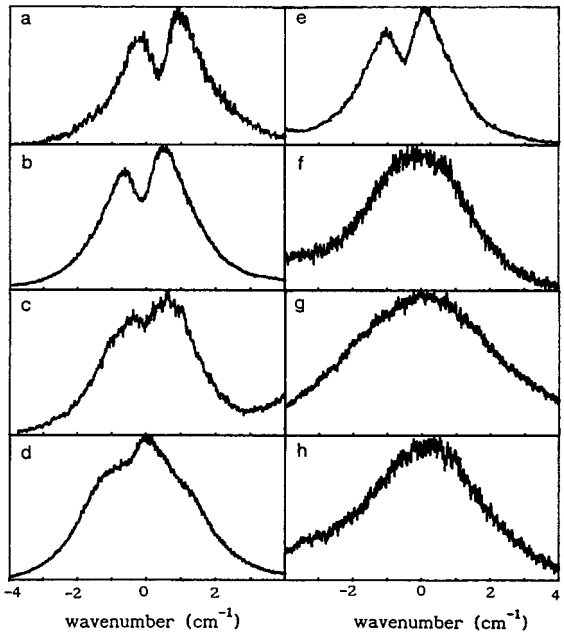

Figure 4. Rotational band contours in the excitation spectrum of DMABN, observed for the band origin $0-0$ (a) and for the transitions at $0-0 + 76$ cm^{-1} (b), $0-0 + 113$ cm^{-1} (c), $0-0 + 136$ cm^{-1} (d), $0-0 + 176$ cm^{-1} (e), $0-0 + 632$ cm^{-1} (f), $0-0 + 916$ cm^{-1} (g), and $0-0 + 1158$ cm^{-1} (h). The laser bandwidth is 0.15 cm^{-1} fwhm. The horizontal scale of each figure covers 8 cm^{-1}.

TABLE 3: Lifetimes of Several Vibronic States in DMABN, Derived from the Linewidths (See Sections 2.4 and 3.3)[a]

excited level (cm^{-1})	contour	Lorentzian line width[b] (cm^{-1})	lifetime[c] (ps)
$0-0 + 76$	*B*	0.3	24(10)
$0-0 + 136$	*C*	0.9	6.5(0.7)
$0-0 + 176$	*B*	0.3	24(10)
$0-0 + 631$	*B*	1.0	5.5(0.5)
$0-0 + 916$	*A*, *B*, or *C*	3.5	1.5(0.06)
$0-0 + 1158$	*B* or *C*	2.5	2.2(0.1)

[a] The spectra are modeled by convolution of a simulated band with a Gaussian (0.16 cm^{-1}) and a Lorentzian representing respectively the instrumental broadening and the lifetime broadening [b] The Lorentzian line width corresponds to the best fit of the model to the measured spectra. [c] In parentheses the errors of the lifetimes are given.

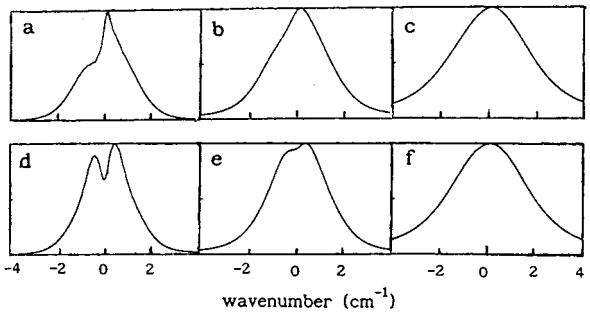

Figure 5. Simulated B- and C-type bands of DMABN with different values for the line width. The line shape is Lorentzian. C-type band: (a) fwhm = 0.3 cm^{-1}; (b) fwhm = 1 cm^{-1}; (c) fwhm = 2.5 cm^{-1}. B-type band: (d) fwhm = 0.3 cm^{-1}; (e) fwhm = 1 cm^{-1}; (f) fwhm = 2.5 cm^{-1}.

From the line width we can obtain information about the dynamic processes in the excited state. If there is no congestion in the bands, the lifetimes can be calculated. These are shown in Table 3. The calculated lifetimes are only meant as approximate values, especially those calculated at higher energies, since the possibility of congestion increases and the type of band

cannot be determined unambiguously. However, the presence of picosecond rapid processes is beyond any doubt.

The values of the lifetimes obtained in this way from the line widths vary from a few to a few tens of picoseconds. This is considerably shorter than the fluorescence decay time of DMABN in the jet, which was found to be 5 ns by Gibson et al.[14,15] They measured the decay of fluorescence observed after excitation of several vibronic states of DMABN in the jet, using the time-correlated single-photon-counting technique (whith a response function of 140 ps; by use of a deconvolution procedure,[25] lifetimes can be extracted down to 50 ps). Throughout the first 1100 cm^{-1} the decay time was found to be 5 ns; no dependence on vibrational excess energy was found. Because of the remarkable difference between their results and ours, we have taken a closer look at their experimental decay curves.[36] The decay is monoexponential, with a lifetime of 5 ns. But in addition, a rapid ingrowth is present, which is not included in the analysis. We estimated the time constant of the ingrowth. The upper limit of this time constant is 50 ps for the state at $0-0 + 176$ cm^{-1}, but it might be shorter.

It seems therefore that the fluorescence is preceded by a rapid intramolecular nonradiative processes. The fluorescence originates from an already "relaxed" state, which is reached on a picosecond time scale. This "relaxed" state has a fluorescence lifetime of about 5 ns.

3.4. Dispersed Fluorescence. In the following we present high-resolution emission spectra of isolated DMABN. The excited-state dynamics will be further discussed in section 4 in connection with the rotational contours of the excitation spectrum.

Figure 6 shows spectra observed after exciting several vibronic levels. A listing of the frequencies is given in Table 4. An abundance of transitions in emission is already present upon exciting the $0-0$ band. The congestion in all emission spectra inhibits a complete assignment. The congestion will be discussed in section 4.

The relatively strong peaks at 440, 800, and 830 cm^{-1} from the excitation energy, as well as the possible overtones at 1560 and 1610 cm^{-1} upon exciting the transitions $0-0 + 136$ cm^{-1} and $0-0 + 176$ cm^{-1}, are probably connected with ring vibrations. The spectra obtained upon excitation of the bands at $0-0 + 76$ cm^{-1}, $0-0 + 113$ cm^{-1}, and $0-0 + 176$ cm^{-1} (all B-type bands) have different relative peak intensities. The emission becomes severely congested upon exciting transitions at higher vibrational excess energy ($0-0 + 632$, $0-0 + 916$, $0-0 + 1160$ cm^{-1}). After excitation at $0-0 + 632$ cm^{-1} only one band at 470 cm^{-1} can be clearly distinguished, while upon excitation at $0-0 + 916$ cm^{-1} a weaker band at 750 cm^{-1} is present. When the $0-0 + 1158$ cm^{-1} is excited, the emission is almost structureless. Excitation in the three last-mentioned transitions, $0-0 + 632$ cm^{-1}, $0-0 + 916$ cm^{-1}, and $0-0 + 1158$ cm^{-1}, associated with ring vibrations, should give rise to recognizable patterns in the fluorescence spectra if no other processes than direct fluorescence from the excited state takes place.

The congestion in the fluorescence spectra indicates that the fluorescence is not directly originating from the primarily excited state.

4. Discussion

The results of the experiments on isolated DMABN, as described above, indicate that the primarily excited electronic state interacts with at least one other nearby electronic state. Grabowski et al.[37] proposed a superposition of transitions involving different electronic states to explain the mixed polarization of vibronic transitions in a glassy solution of DMABN. In their experiments the observed transitions differ significantly in the direction of their transition dipole moments. According to these authors, this is due to vibronic coupling to closely situated excited states.

From rotational contour analysis of bands near the origin of the LIF excitation spectrum we have deduced that the conformation of DMABN in the initially excited electronic state differs only slightly from the ground-state conformation. One would therefore expect a sort of mirror image between excitation and

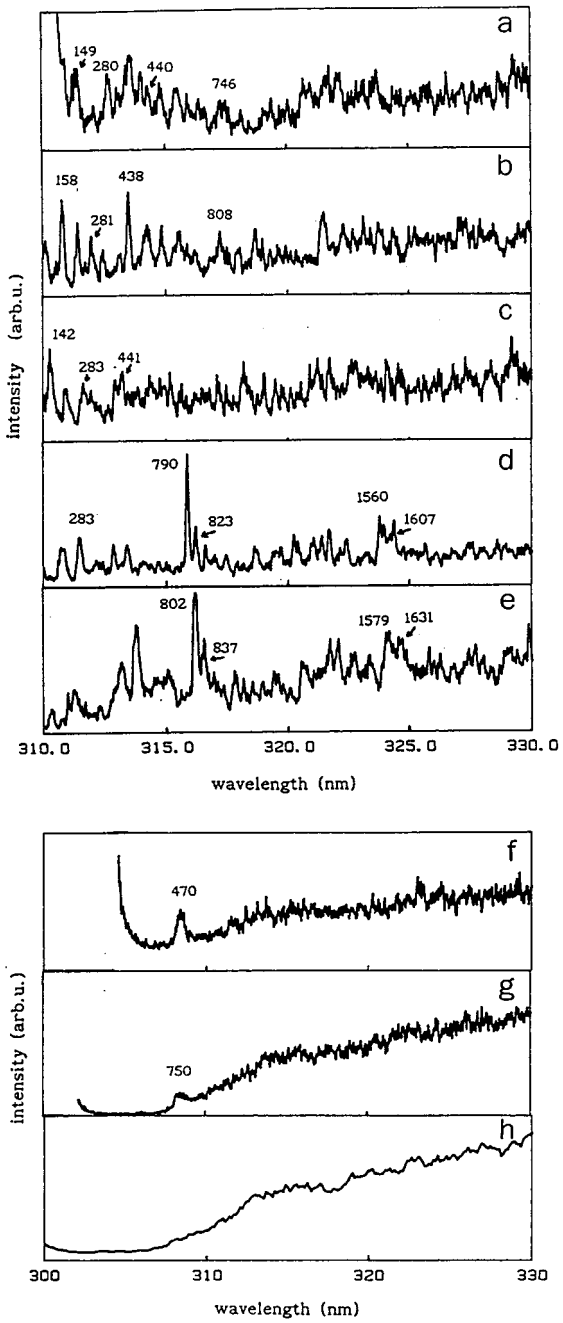

Figure 6. Dispersed fluorescence spectra of DMABN upon excitation of the following transitions: (a) the origin $0-0$, (b) $0-0 + 76$ cm^{-1}, (c) $0-0 + 113$ cm^{-1}, (d) $0-0 + 136$ cm^{-1}, (e) $0-0 + 176$ cm^{-1}, (f) $0-0 + 632$ cm^{-1}, (g) $0-0 + 916$ cm^{-1}, (h) $0-0 + 1158$ cm^{-1}. (a)–(c) and (e) were taken at a monochromator resolution of 17 cm^{-1}, while (d) was taken at 8 cm^{-1} and (f) and (g) at 41 cm^{-1}. The intensity at and near the resonance energy is mainly due to scattered laser light. The peaks in the spectra are denoted by their separation in wavenumbers (cm^{-1}) with respect to their excitation frequency.

TABLE 4: Relative Peak Positions (in cm^{-1}) in the Dispersed Fluorescence of DMABN after Excitation of Single Vibronic Levels near the Electronic Origin[a]

0_0^0	0_0^0+76		0_0^0+113		0_0^0+136		0_0^0+176	
Δ_{exc}	Δ_{exc}	Δ_{rel}	Δ_{exc}	Δ_{rel}	Δ_{exc}	Δ_{rel}	Δ_{exc}	Δ_{rel}
								−96
						−56		−48
				−26		−8		
(0)		14		29				35
		82	87		80	68	80	
97	90			97				
149	158	148	142		128		128	133
						170		
		205	210	207	204		211	
218	224	254				222		
280	281		283	272	283	280	309	
				303				
	330	324		328				328 (br)
368		362	385		358	358		389
416	400		416		416	414		
440	438	438	441					
494		496			494		504 (br)	
	514							
559	572	566			550		565	
	642					654		626
								661
746		732			790	687	802	
	808			830	823		837	
		877						
	953		943					
		1152						
	1228							
						1424		1403
					1560	1471	1579	1454
					1607		1630	

[a] The values of Δ_{exc} have been obtained by subtracting the peak frequency from the excitation frequency, and Δ_{rel} is the difference between the frequency of the 0_0^0 transition (32 246.5 cm^{-1}) and the frequency of the peak.

emission spectra. However, the emission spectra obtained after excitation of several vibronic levels (cf., Figure 6) bear very little resemblance to the LIF excitation spectrum. No indication of any mirror-image relation can be found. The striking differences between the various emission spectra and between the excitation spectrum suggest that the initially excited state is not the (only) emitting state. Internal conversion (IC) following the excitation process could bring about the observed differences between the spectra, in particular when the equilibrium conformations of the initially excited state and the emitting state are different.

Because of the lack of mirror symmetry between the LIF excitation spectrum (Figure 1) and the emission spectrum (Figure 6a) obtained upon excitation of the band at 310.022 nm (the first band in the excitation spectrum), it is not certain that this transition is in fact the 0−0 transition. But if it actually is the 0−0 transition, excitation via this band could be followed by an IC process in which the vibrationless level of the (optically accessible) S_1 state is converted into vibronic levels belonging to some excited electronic state S_x with a lower potential energy minimum. The equilibrium conformations of S_1 and S_x are different along the coordinate of a particular mode *m*. Vibronic transitions $S_0 \rightarrow S_x$ will contribute, at higher excitation energies, to the excitation spectrum $S_0 \rightarrow S_1$, but if the corresponding Franck−Condon factors for mode *m* are low, this would give rise only to a weak background. We assume that the vibronic states of S_x, produced by IC, are composed of spectrally inactive vibrations that do not change their quantum numbers v_i during the transition $S_x \rightarrow S_0$ ($\Delta v_i = 0$). The vibrational structure in the fluorescence spectrum is due to transitions $\Delta v_a \neq 0$ of spectrally active modes. Figure 6 shows that the fluorescence spectra obtained after excitation of the single vibronic levels at 0−0 + 176 cm^{-1}, 0−0 + 113 cm^{-1}, etc. are strikingly different. This corroborates our conclusion that the initially excited level is depopulated by a fast nonradiative process that leads to the formation of a different emitting state. If the fluorescence originates exclusively from the primarily excited levels, the spectra in Figure 6 should show similar vibrational progressions but with different spectral origins. However, the frequency spacings show many differences, and the intensity distributions are even markedly different, as can be seen.

Internal conversion between S_1 and S_x could be a fast process because of the small energy gap between both states. In general, IC between excited electronic states is much faster than between S_1 and S_0 because the energy gaps between the excited states are considerably smaller. Time constants in the picosecond and subpicosecond region have been found for S_2-S_1 internal conversion in large molecules such as phenanthrene,[38] porphyrines and porphine,[39] and tetraenes,[40] while the S_1-S_0 conversion proceeds on a nanosecond time scale. For the dynamic properties of the excited electronic states of DMABN the dimethylamino moiety will be important. It is involved in a number of low-frequency motions. We can distinguish internal rotations of the dimethylamino moiety and also of both methyl groups separately, as well as the inversion motion of the dimethylamino group. In this respect it is interesting to compare the properties of 4-aminobenzonitrile (ABN) and DMABN. ABN lacks the methyl groups on the amino moiety. As a consequence, both the inversion mode and the torsional mode in ABN have higher frequencies than in DMABN. In the LIF excitation of jet-cooled ABN, measured by Gibson et al.,[14] all transitions are B type. Excitation into these peaks gives rise to structured fluorescence, which can be attributed to the primarily excited level.

To explain the spectroscopic properties of DMABN, we assume (i) the presence of an excited electronic state S_x with a lower energy minimum than S_1 and with a different equilibrium geometry and (ii) fast internal conversion between the optically excited S_1 state and S_x. The low-frequency motions in DMABN will contribute considerably to the density of vibronic states, even at relatively low excess energies, and therefore, these vibrational modes are likely to advance the IC process. Parmenter and co-workers[41] showed convincingly by comparing *p*-fluorotoluene with *p*-difluorobenzene that the presence of a methyl group greatly enhances both the rate of intramolecular vibrational-energy redistribution (IVR) and the number of IVR channels. We propose that S_1 and S_x interchange their relative positions when the molecule is distorted along the coordinate of some (large-amplitude) mode *m*. An interchange of electronic states upon distortion along the coordinate of the torsional mode was proposed by Grabowski and co-workers[3] to explain the phenomenon of strongly red-shifted fluorescence of DMABN in polar solvents.

By virtue of the spectroscopic data discussed above, there is no compelling reason to assume that the proposed interchange of the electronic states S_1 and S_x in DMABN is connected with variations in the twist angle; it is, however, possible. Other molecular variables could be involved in mode *m*, which is assumed to be related to the interchange of S_1 and S_x. Furthermore, it should be realized that, in addition to S_x, other electronic states could be situated very close to S_1. The estimated lifetimes of the levels belonging to the B-type transitions decrease with increasing excess vibrational energy. We think that the lifetimes of these levels are determined by internal conversion, as discussed above. This would explain why the lifetimes decrease with increasing vibrational energy, as a consequence of an increasing level density in the accepting vibronic manifold.

The appearance of a C-type transition ($0-0 + 136$ cm^{-1}) together with a number of adjacent B-type transitions in the LIF excitation spectrum presents another indication of the complex nature of the excited states. Also, the estimated lifetime of the level at $0-0 + 136$ cm^{-1} is not in line with those of the adjacent levels. This particular level might obtain its deviant properties as a result of vibronic coupling. According to the calculations of Lipinski,[20] the transition belonging to the TICT state should give rise to an A-type contour; such a transition is in the plane of the molecule and polarized along the long axis. We conclude therefore that the C-type transition is not directly related to the TICT state, but it could be connected to the TICT state via another electronic state. It should be mentioned that these results are supported by the theoretical work of Serrano-Andres et al.;[23] their calculations show that a small energy gap between the interacting states is necessary for the occurrence of dual fluorescence and TICT in aminobenzonitriles.

In DMABN, owing to its low-frequency motions, only little energy is necessary to change the position of the dimethylamino group with respect to the benzonitrile part. One of the large-amplitude motions is directly connected with the TICT process, namely, the twist motion of the dimethylamino group. Both the high density of states that accompany these low-frequency motions and the possibility of bringing about conformational changes facilitate the internal conversion. Internal conversion can be considered a precondition for the occurrence of TICT.

5. Conclusions

The work described in this paper indicates that the fluorescence from isolated DMABN molecules originates from coupled electronic states. Rotational contour analysis of several transitions in the LIF excitation spectrum reveals a complex picture of the excited state. The origin band of the excitation spectrum and several transitions nearby have a double-headed B-type contour. The transitions are polarized in the molecular plane, which is indicative of a $\pi\pi^*$ excited state. The planar geometry of DMABN in the ground state is retained in the excited state. The dimethylamino group, which is coplanar with the benzonitrile plane, maintains this orientation in the B-type transitions. No big changes in bond lengths have been found. In the LIF excitation spectrum low-frequency modes are active. Apparently, electronic excitation produces small displacements along the coordinates of these low-frequency modes. However, these displacements are too small to be inferred from the rotational contour analysis.

At $0-0 + 136$ cm^{-1} a C-type band is found. This transition is polarized perpendicular to the molecular plane, and most likely, it is of $n\pi^*$ character. The rotational contour of this band can only be simulated with a great change in the equilibrium value of the twist angle of the dimethylamino group, viz. from 0° in the ground state to about 90° in the excited state. Therefore, we assume that the dimethylamino group is involved in the electronic transition. The transition will be probably from the lone pair of the nitrogen to the benzonitrile π-electron cloud and will have charge-transfer character. Transition to the cyano group, as suggested by Hashimoto et al.,[5] is, however, also possible.

From the rotational contour analysis an indication of the lifetimes of the excited levels is obtained. These estimated lifetimes vary from about 24 ps to less than 2 ps. In our view the lifetimes of these levels are determined by an internal conversion process in which the initially excited state is converted into another excited electronic state with a lower energy minimum. As a consequence, the primarily excited electronic state is not the (only) emitting state. This would explain the lack of mirror symmetry between the LIF excitation spectrum (Figure 1) and the emission spectra (Figure 6), as well as the differences between the various single-vibronic level emission spectra.

In conclusion, the excited state of isolated, supercooled DMABN consists of a potential energy surface in which several electronic states and vibrations are mutually connected and interacting. We show the presence of B- and C-type transitions in the excited state of DMABN with different conformations. The broadening of the rotational lines, in combination with analysis of the dispersed fluorescence spectra, indicates that the fluorescence is preceded by a fast radiationless intramolecular process (internal conversion) on a picosecond time scale.

Acknowledgment. We express our thanks to Ing. D. Bebelaar for technical help. Prof.dr. Z.R. Grabowski is kindly acknowledged for initiating this work. This work is supported by The Netherlands Foundation for Chemical Research (SON). The Netherlands Organization for Scientific Research (NWO) is kindly acknowledged for financial aid to F. Pérez Salgado and J. Herbich. This work is partly done within the Polish research program CPBP 01.19 and RP II.13.

References and Notes

(1) Lippert, E.; Luder, W.; Boos, H. In *Advances in Molecular Spectroscopy*; Mangini, A., Ed.; Pergamon Press: Oxford, 1962; p 443.

(2) Rotkiewicz, K.; Grellmann, K. H.; Grabowski, Z. R. *Chem. Phys. Lett.* **1973**, *19*, 315.

(3) Grabowski, Z. R.; Dobkowski, J. *Pure Appl. Chem.* **1983**, *55*, 245. Herbich, J.; Grabowski, Z. R.; Wojtowicz, H.; Golankiewicz, K. *J. Phys. Chem.* **1989**, *91*, 3491. Grabowski, Z. R.; Rotkiewicz, K.; Siemiarczuk, A.

J. Lumin. **1979** *18/19*, 420. Grabowski, Z. R.; Dobkowski, J.; Kuhnle, W. *J. Mol. Struct.* **1984**, *114*, 93. Grabowski, Z. R. *Pure Appl. Chem.* **1993**, *65*, 1751.

(4) Okada, T.; Mataga, N.; Baumann, W.; Siemiarczuk, A. *J. Phys. Chem.* **1987**, *91*, 4490. Rettig, W.; Wermuth, A.; Lippert, E. *Ber. Bunsen-Ges. Phys. Chem.* **1979**, *83*, 692. Grabowski, Z. R.; Rotkiewicz, K.; Krowczynski, K.; Cowley, D. J.; Baumann, W. *Nouv. J. Chim.* **1979**, *3*, 443. Wang, Y.; Eisenthal, K. B. *J. Chem. Phys.* **1982**, *77*, 6076. Visser, R. J.; Weisenborn, P. C. M.; Varma, C. A. G. O.; de Haas, P. M.; Warman, J. M. *Chem. Phys. Lett.* ***1984****, 104, 38*. Rettig, W.; Wermuth, G. *J. Photochem.* **1985**, *28*, 351.

(5) Hashimoto, M.; Hamaguchi, H. *J. Phys. Chem.* **1995**, *99*, 7875.

(6) Kajimoto, O.; Nsayuki, T.; Kobayashi, T. *Chem. Phys. Lett.* **1993**, *209*, 357.

(7) Schuddeboom, W.; Jonker, S. A.; Warman, J. M.; Leinhos, U.; Kuhnle, W.; Zachariasse, K. A. *J. Phys. Chem.* **1992**, *96*, 10809. Zachariasse, K. A.; von der Haar, Th.; Leinhos, U.; Kuhnle, W. *J. Inf. Rec. Mater.* **1994**, *21*, 501.

(8) Herbich, J.; Pérez Salgado, F.; Rettschnick, R. P. H.; Grabowski, Z. R.; Wojtowicz, H. *J. Phys. Chem.* **1991**, *95*, 3491. Warren, J. A.; Bernstein, E. R.; Seeman, I. *J. Chem. Phys.* **1987**, *88*, 871. Kajimoto, O.; Yokoyama, H.; Oshima, Y.; Endo, Y. *Chem. Phys. Lett.* **1989**, *179*, 455.

(9) Kobayashi, T.; Futakami, M.; Kajimoto, O. *Chem. Phys. Lett.* **1987**, *141*, 450. Rotkiewicz, K.; Rubaszewska, W. *J. Lumin.* **1982**, *27*, 221.

(10) Peng, L. W.; Dantus, M.; Zewail, A. H.; Kenmitz, K.; Hicks, J. M.; Eisenthal, K. B. *J. Phys. Chem.* **1987**, *91*, 6162.

(11) Howell, R.; Phillips, D.; Petek, H.; Yoshihara, K. *Chem. Phys.* **1994**, *199*, 303.

(12) Howells, B. R.; McCombie, J.; Palmer, T. F.; Simons, J. P.; Walters, A. *J. Chem. Soc., Faraday Trans.* **1992**, *88*, 2595.

(13) Kobayashi, T.; Futakami, M.; Kajimoto, O. *Chem. Phys. Lett.* **1986**, *130*, 63.

(14) Gibson, E. M.; Jones, A. C.; Phillips, D. *Chem. Phys. Lett.* **1987**, *136*, 454.

(15) Gibson, E. M.; Jones, A. C.; Phillips, D.; Taylor, A. G.; Bouwman, W. G.; Sandell, D. *J. Phys. Chem.* **1988**, *92*, 5449.

(16) Grassian, V. H.; Warren, J. A.; Bernstein, E. R.; Secor, H. V. *J. Chem. Phys.* **1989**, *90*, 3994.

(17) Kajimoto, O.; Yokoyama, H.; Ooshima, Y.; Endo, Y. *Chem. Phys. Lett.* **1991**, *179*, 455.

(18) Heine, A.; Herbst-Irmer, R.; Stalke, D.; Kühnle, W.; Zachariasse, K. A. *Acta Crystallogr.* **1994**, *B50*, 363.

(19) Gourdon, A.; Launay, J.; Bujoli-Doeuff, M.; Heisel, F.; Miehé, J. A.; Amouyal, E.; Boillot, M. *J. Photochem. Photobiol. A* **1993**, *71*, 13.

(20) Lipinski, J.; Chojnacki, H.; Grabowski, Z. R.; Rotkiewicz, K. *Chem. Phys. Lett.* **1980**, *70*, 449. Visser, R. J.; Varma, C. A. G. O.; Konijnenberg, J.; Bergwert, P. *J. Chem. Soc., Faraday Trans.* **1983**, *2*, 79, 347. Cowley, D. L.; Peoples, A. H. *J. Chem. Soc., Chem. Commun.* **1977**, 352. Lewis, F. D.; Holman, B. *J. Phys. Chem.* **1980**, *84*, 2326. Khalil, O. S.; Meeks, J. L.; McGlynn, S. P. *Chem. Phys. Lett.* **1976**, *39*, 457.

(21) Rettig, W.; Bonacic-Koutecky, V. *Chem. Phys. Lett.* **1979**, *62*, 115.

(22) Kato, S.; Amamatsu, Y. *J. Chem. Phys.* **1990**, *92*, 7241.

(23) Serrano-Andres, L.; Merchan, M.; Roos, B. O.; Lindh, R. *J. Am. Chem. Soc.* **1995**, *117*, 3189.

(24) Perez Salgado, F. Ph.D. Thesis, University of Amsterdam, The Netherlands, 1992.

(25) Kunst, A. G. M. Ph.D. Thesis, University of Amsterdam, The Netherlands, 1992.

(26) Smalley, R. E.; Wharton, L.; Levy, D. H. *J. Mol. Spectrosc.* **1977**, *66*, 375. Job, V. A.; Innes, K. K. *J. Mol. Spectrosc.* **1978**, *71*, 299.

(27) Haynam, C. A.; Brumbaugh, D. V.; Levy, D. H. *J. Chem. Phys.* **1984**, *80*, 2256. Kunst, A. G. M. Ph.D. Thesis, University of Amsterdam, 1992.

(28) Kobayashi, T.; Honma, K.; Kajimoto, O.; Tsuchiya, S. *J. Chem. Phys.* **1987**, *86*, 1111.

(29) Yamanouchi, K.; Watanabe, H.; Koda, S.; Tsuchiya, S. *Chem. Phys. Lett.* **1984**, *107*, 290.

(30) Christofferen, J.; Hollas, J. M.; Kirby, G. H. *Mol. Phys.* **1969**, *16*, 441.

(31) Bixon, M.; Jortner, J. *J. Chem. Phys.* **1968**, *48*, 715.

(32) Brand, J. C. D.; Knight, P. D. *J. Mol. Spectrosc.* **1970**, *36*, 328.

(33) Gordon, R. D.; Clark, D.; Crawley, J.; Mitchell, R. *Spectrochim. Acta* **1984**, *40A*, 657.

(34) Thakur, S. N.; Tiwari, S. K.; Rai, D. K. *J. Mol. Struct.* **1970**, *5*, 309.

(35) The bands at higher excess energy in Table 3 could not be simulated using a fwhm of 0.3 cm^{-1} (Gaussian or Lorentzian) and a single band type. Simulations were performed by mixing of A-, B-, and C-type transitions (with twist angles of 0° and 90°) to check hybrid bands. The following percentages of mixing of A- and B-type bands and of B- and C-type bands were used: 25%, 50%, and 75% of the B-type (these percentages refer to the integrated area of each band). Gaussian and Lorentzian line profiles (0.3 cm^{-1}) were used. In all cases, the bands could not be reproduced using a hybrid band with a width of 0.3 cm^{-1}. To simulate a congested band, we superimposed several bands (up to five) of the same type, at different distances with respect to each other (0.1, 0.25, and 0.5 cm^{-1}). The superpositions could not fit the observed contours. In conclusion, only good fits were obtained in the simulations using single band types with relatively high values for the bandwidth (>0.3 cm^{-1}).

(36) Gibson, E. M. Ph.D. Thesis, London, 1989.

(37) Grabowski, Z. R.; Rotkiewicz, K.; Rubaszewska, W.; Kirkor-Kaminska, E. *Acta Phys. Pol.* **1978**, *A54*, 767.

(38) Amirav, A.; Sonnenschein, M.; Jortner, J. *J. Phys. Chem.* **1984**, *88*, 5593.

(39) Even, U.; Magen, J.; Jortner, J.; Friedman, J.; Levanon, H. *J. Chem. Phys.* **1982**, *77*, 4374. Even, U.; Magen, J.; Jortner, J.; Friedman, J. *J. Chem. Phys.* **1982**, *77*, 4384. Even, U.; Jortner, J. *J. Chem. Phys.* **1982**, *77*, 4391.

(40) Bouwman, W. G.; Jones, A. C.; Phillips, D.; Thibodeau, P.; Friel, C.; Christensen, R. L. *J. Phys. Chem.* **1990**, *94*, 7429.

(41) Hotzclaw, K. W.; Parmenter, C. S. *J. Phys. Chem.* **1984**, *88*, 3182. Parmenter, C. S.; Stone, B. M. *J. Chem. Phys.* **1986**, *84*, 4170. Moss, D. B.; Parmenter, C. S.; Ewing, G. E. *J. Chem. Phys.* **1987**, *81*, 51.